Department of Geography
College of Science
P.O. Box 443025, University of Idaho
Moscow, ID 83844-3025

SCIENTIFIC AREA:     **Earth Sciences (Global Change)**

PROJECT TITLE:

# PALEO-CLIMATIC and ENVIRONMENTAL ICE CORE RESEARCH, DATA ANALYSIS and INTERPRETATION
(mid- low- latitudes, high altitudes glaciers at the Northern Hemisphere)

PI:     **Vladimir B. Aizen**
CONTACT:     Tel: 208-885-5888, fax: 208-885-5724, e-mail: aizen@uidaho.edu

## FINAL   REPORT

**DOE/INEEL Contract Number: BBWI 00000073 R10**
**Budget Period: 01/10/2003 to 30/09/2005**

*14 December, 2005*

RESEARCH  TEAM, FY2004/2005:

Professor, Dr. **Vladimir B. Aizen**, glaciologist
Department of Geography, College of Mines and Earth Resources,
P.O. Box 443025, University of Idaho
Moscow, ID 83844-3025, **U.S.A.**
Tel. (208) 885-5888, fax. (208) 885-5724
E-mail: aizen@uidaho.edu

Associate Researcher, Dr. **Elena M. Aizen**, climatologist
Department of Geography, College of Mines and Earth Resources,
P.O. Box 443025, University of Idaho
Moscow, ID 83844-3025, **U.S.A.**
Tel. (208) 885-5888, fax. (208) 885-5724
E-mail: eaizen@uidaho.edu

Professor, Dr. **John D. Marshall**, Director: Idaho Stable Isotopes
Laboratory, College of Natural Resources, P.O. Box 441133,
Moscow, ID  83844-1133, **U.S.A**.
Tel. (208) 885-6695, fax. (208) 885-6226
E-mail: jdm@uidaho.edu

Assistan Professor, Dr. **Nazomu Takeuchi**
Research Institute for Humanity and Nature, 335 Takashima-cho,
Kamigyo-ku, Kyoto 602-0878, **Japan**
Tel. +81 (0) 75-229-6177, fax. +81 (0) 75-229-6150
E-mail: takeuchi@chikyu.ac.jp

Professor, Dr. **Stanislav A. Nikitin**, geophysicist
Glacio-Climatological Laboratory, Tomsk State University, 36
Lenina Str., Tomsk 634050, **Russian Federation**
Tel. +7 (3822) 55-47-03, fax. +7 (3822) 41-58-92
E-mail: nikitin@ic.tsu.ru

Professor, Dr. **Alexander S. Finaev**, geophysicist
Institute of Water Resources and Hydropower National Academy
of Sciences of the Tajikistan. 106 Rudaki Ave., Dushanbe,
734025, **Tajikistan**.
Tel. +992 (372) 24-44-50. E-mail: foker@list.ru

Rober Brander a technician from the Stable Isotope Laboratory of the University of Idhao, two graduate students (Daniel Joswiak and Arzhan Surazakov) and two undergraduate students (Brian Andersen and Christy Schwartz) from the University of Idaho, two graduate students from the University of Maine (Susan Kaspari and Bjorn Griholm), and two graduate students from the Research Institute for Humanity and Nature (Jun Miyake and Tsutomu Kadota) were also involved in field and laboratory research during FY2004/2005.

**Table of Contents:**

**PREFACE**

More than half of the Earth's surface area lies in the low-mid latitudes of the Northern Hemisphere. Thus, temporal and spatial variability in climate and environmental change in these temperate and tropical zones is of global importance. However, instrumented records of climate and environmental variability barely covers the last 100 years and throughout portions of the Asian continent is sparse if not totally absent. Ice cores from mid- low- latitude glaciers can provide high-resolution records of past climate dynamics, and chemistry of the atmosphere and terrestrial systems extending back in time on annual to centennial time-scales (*Adhikary et al., 1995; ICARA, 2005; IPICS, 2005*). However, mid-low latitudes high-elevation glaciers suitable for the preservation of robust climate and environmental change records are rapidly disappearing as a consequence of greenhouse gas warming. Fortunately, there are still high elevation glaciers situated over the great Eurasian continent from which such records can still be retrieved.

The primary aim of our research is to develop and interpret an array of Asian ice core records that robustly capture past climate and environmental change. The ice core array is comprised of:

(1) Four cores (>50m deep) and another seven (<50m deep) that have already been collected and partly analyzed (Fig 1).
(2) Six new cores (150-1000m deep) that we propose to recover and analyze from new sites (Fig 1).

The six new cores will expand notably the east-west and the north-south spatial coverage of ice cores over central Asia (Fig. 1). The rationale underlying the investigation of this array of Asian ice cores is similar to that underlying the highly successful ice core array largely completed over Antarctica as part of the International Trans Antarctic Scientific Expedition (ITASE, 1997). The rationale represents the logical "raising of the scientific bar" from single to array core coverage. The Asian ice core array provide, as ITASE does for Antarctica, 200-10,000+ year long records that capture the spatial and the decadal to centennial scale temporal complexity of continental-scale climate and environmental variability.
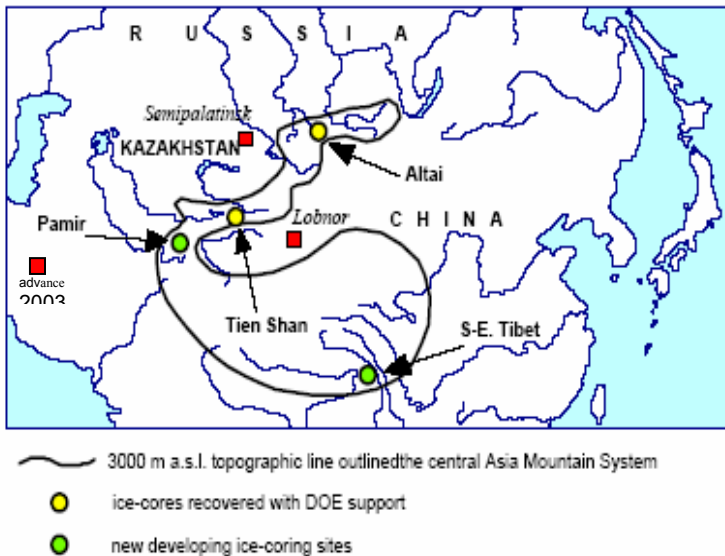


*Fig*. *1.* *Four ice-coreing sites developed during the Project*
🟥 *nuclear poligons*

The time period 200-1000+ years is chosen for the Asian ice core array in order to assure at least 100 years more than the period of instrumented record length (~AD 10,000) and to predate the era of anthropogenic involvement in climate change. The depth of most Asian ice cores (100-300m) typically precludes detailed annual layer counting in excess of ~500 years although multi-annual interpretation of records can be extended using flow modeling to at least 1000 years ago. However, record lengths in the range of the last 10,000 years allow inclusion of the era classically containing the Little Ice Age (onset ~AD1400) and Medieval Warm Period – the most recent analogs for naturally cold and warm temperatures. The LIA/MWP transition is marked by abrupt change in portions of the Northern Hemisphere (Mayewski et al., 2005). The six new cores are all expected to provide annually dated records of at least 300-5000 years and at lower resolution back to ~10,000 years based on known accumulation rates and ice depths at the selected sites.

The Eurasian continent is the largest landmass in the World, exerting substantial influence on atmospheric and terrestrial systems. It is a diverse region, covered by tundra, boreal/tropical forests, semi-deserts and deserts, holding more than two-thirds of the land on Earth that is underlain by permanent soil ice or permafrost. The greatest highlands in the World: the Himalayas, Karakoram, Hindu Kush, Tibetan Plateau, Pamir, Tien Shan, and Altai mountains define the Asian Mountain System (AMS). The AMS has an area of ~6 million $km^2$, more than 100,000 glaciers with a total area of >115,000 $km^2$ comprising ~11,000 $km^3$ of fresh water that is a vital source of life for 2.5 billion people living in the mountains and surrounding terrain. Changes in atmospheric circulation over the AMS impact water resources over this heavily populated region and may cause unpredictable consequences all over the World.

Asian meteorology is controlled by polar air masses from the Arctic, continental air masses from central Asia, and maritime air masses from the Pacific and Indian Ocean (Bryson, 1986). Thus, a spatially distributed array of ice cores from Asia is essential to understanding the regional differences in atmospheric circulation and Asian climate in general. As an example, the Central and South Asian region, encompassing the Tibetan Plateau and Himalayas, has an extremely dynamic climate system that plays a significant role in modulating global climate. The Tibetan Plateau is roughly 3500 by 1500 kilometers in size, has an average elevation of ~5000 m, and contains the largest concentration of the world's snow and ice outside of Antarctica and Greenland. The Himalayas to the south contain all of the world's peaks higher than 8000 m and hundreds of >7000 m peaks. Due to its massive size and high elevation, the Tibetan Plateau and Himalayan region influences the distribution of surface and upper-level atmospheric pressure via seasonal heating and cooling and splitting of the upper-level westerlies (Fig 2). The extreme relief of the region produces large-scale standing waves (Rossby waves) within the upper atmosphere (>500 mb) of the Northern Hemisphere. The large elevation differences between the Himalayas and the ocean increase the effects of the large



Fig. 2. *Study locations at the northern and southern periphery of the Asian mountain system with the main trajectories of air masses that bring moisture to them.*

land/sea heat differential thus contributing to the South Asian monsoon, the largest seasonal reversal of wind patterns and precipitation regimes on the planet. The Asian monsoon affects roughly one quarter of Earth's population. Extensive research on modern monsoon variability has established links between South Asian monsoon strength and sea surface temperature anomalies, Eurasian snow cover, and the El Niño Southern Oscillation (ENSO). However, understanding of the South Asian monsoon variability on interannual and longer time-scales is limited due to the relatively short length of the instrumental record in Asia (~100 years and sparse).
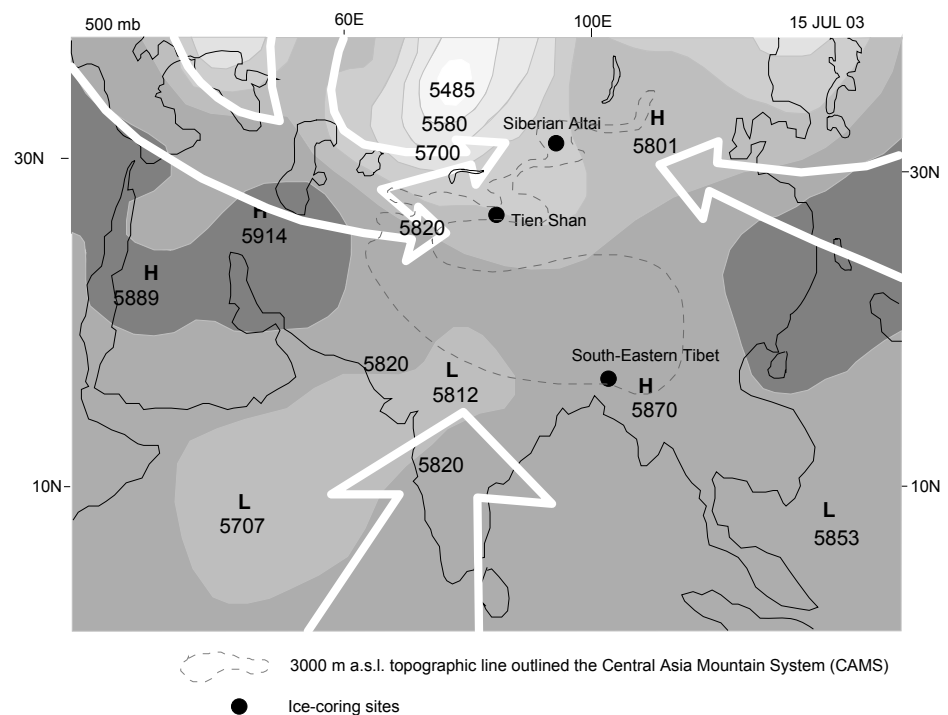
To develop a composite view of past, modern and future climate variability over Asia and to define, for example, the interaction over time between the westerly jet stream and the Asian monsoon, it is critical to link an array of well-dated, high-resolution, continuous, multi-variate, instrumentally-calibrated ice core records from mid-low latitude glaciers and compare these records with polar ice core information. Ice cores are archives of past atmospheric and environmental conditions, and preserve information about the natural and anthropogenic atmospheric content, atmospheric circulation, and aerosol and contaminant transport and deposition. Chemical and physical analyses of firn/ice cores recovered from carefully selected accumulation zones of Asian glaciers provide high-resolution paleoclimate and environmental records. Since the 1980's glaciochemical records have been recovered from numerous high mountain sites in central Asia (*e.g., Mayewski et al., 1981, 1984; Lyons and Mayewski, 1983; Lyons et al., 1991; Wake et al., 1990, 1993, 1994, 2004; Thompson et al., 1989, 1990, 1995, 2000; Williams et al., 1992; Kang et al, 2000, 2001, 2002; Kreutz and Sholkovitz, 2000; Kreutz et al., 2000, 2001, Olivier et al., 2003; Aizen et al, 2004, 2005*).

Climate in the Himalayas is strongly influenced by the Asian Monsoon, and ice cores from this region are characterized by very low ion burdens representative of relatively clean upper tropospheric air. Conversely, climate records from ice cores collected in the central and northern regions of the Tibetan plateau are dominated by dust derived from the arid regions of central Asia (e.g. Taklamakan and Qaidam deserts), and have higher ion burdens (*Wake et al., 1990, 1993, 2004; Kang et al., 2002, 2003*). The remote areas of the Tibetan Plateau and Himalayas are generally regarded as pristine and relatively devoid of contamination, however recently industrial pollutants (organic compounds from petroleum residues and oxalate) have been identified in Himalayan snow (*Xie et al., 2000, Kang et al., 2001 a, b*). Additionally, analysis of ice cores from our work on Mt. Everest indicates a sharp increase in ammonium concentrations since the 1940's that may be related to enhanced agricultural activities, (*Kang et al., 2002; Hou et al., 2003; Qin et al., 2002*) and ice cores from Mt. Everest and Dasoupu show an increasing trend to higher sulfate and nitrate concentrations (*Qin et al., 2002; Thompson et al., 2000*) that may be related, as proposed earlier, to increased biomass burning (*Davidson et al., 1986*) or local acidic gases (*Shrestha et al., 1997*). These records indicate that anthropogenic activity is altering the atmospheric chemistry in remote regions, but interpretation of the records can be complicated because some contaminants (heavy metals and organic species) have natural and anthropogenic sources and changes in circulation can lead to the redistribution of pollutants. The history of deposition for most contaminants is incomplete, thus more detailed records are needed to assess the anthropogenic contributions to the remote atmosphere over central Asia.

High Asian glaciers are sensitive indicators of climate change. A 0.6°C increase in global temperature since 1950 has contributed to the widespread melting of low latitude, high elevation glaciers. Loss of these glaciers threatens the water resources necessary for many populations. Once the glaciers melt paleoclimatic archives that are preserved within the ice are lost forever (*ICARA, 2005*). It is a high priority to collect these records to determine the emission history of natural and anthropogenic atmospheric constituents, and to investigate the long-term variability of climate. It should be noted that not all glaciers are undergoing retreat (e.g., many glaciers in the Geladandong region, Fig 1), and that the response of glaciers to climate change is variable as a consequence of the balance between temperature and accumulation rate on varying spatial and temporal scales.

Our research is a multi-disciplinary, multi-institutional, international effort. In this report, we present some results of our resent results received in FY2004/2005. All theis research was conducted under the Project: 'Paleo-Climatic and Environmental Ice Core Research, Data Analysis and Interpretation in Asia Mountains'.

## PART I. CLIMATIC AND ATMOSPHERIC CIRCULATION PATTERN VARIABILITY FROM ICE-CORE ISOTOPE/GEOCHEMISTRY RECORDS (ALTAI, TIEN SHAN AND TIBET)

### Overview
### Major and REE Concentrations in the Pamir firn core

In 2001, 2002 and 2003 several firn/ice cores were recovered from the Siberian Altai (Belukha), Central Tien Shan (Inilchek Gl.) and the South-Eastern Tibet (Zuoqiupu Gl, Bomi) from 1998 to 2003. The comparison analyses of stable isotope/geochemistry records obtained from these firn/ice cores identified the physical links controlling the climate related signals at the seasonal scale variability. The core data related to physical stratigraphy, meteorology and synoptic atmospheric dynamics were the basis for calibration, validation and clustering of the relationships between the firn/ice cores isotope/geo-chemistry and snow accumulation, air temperature and precipitation origin. The mean annual accumulation at the Inilchek Glacier was 106 g cm$^{-2}$ yr$^{-1}$, at Belukha 69 g cm$^{-2}$ yr$^{-1}$, and at Zuoqiupu 196 g cm$^{-2}$ yr$^{-1}$ in w.e. The slopes in regression lines between the $\delta^{18}$O ice core records and air temperature were found to be positive for the Tien Shan and Altai glaciers, and negative for southeastern Tibet, where heavy amounts of isotopically depleted precipitation occur during summer monsoons. The technique of coupling synoptic climatology and meteorological data with $\delta^{18}$O and d-excess in firn core records was developed to determine climate-related signals and to identify the origin of moisture. In Altai, two-thirds of accumulation from 1984 to 2001 was formed from oceanic precipitation and the rest of the precipitation was re-cycled over Aral-Caspian sources. In Tien Shan, 87% of snow accumulation forms by precipitation originated from the Aral-Caspian closed basin, Eastern Mediterranean and Black seas, and 13% from the North Atlantic.

### STUDY REGIONS
### Long-term data:

For determination of isotope/air-temperature relationships, seasonal/monthly calibration of annual accumulation layers in snow/firn/ice cores record were used in conjunction with long-term monthly-averaged meteorological data from stations within 10-150 km of the drill sites and with data from established automated weather stations in the immediate vicinity of the drilling sites. Data from these stations have the highest correlation with air temperature and precipitation time series at the studied glaciers. The long-term average monthly air precipitation and temperature for the period of 1990-2000 at the altitudes of the

**Fig**. *3 Average monthly precipitation (a) and air temperatures (b) corrected with the local seasonal lapse rates to drill site elevations* (Siberian Altai, *4115 m).*

drilling sites (Fig. 3a, b) were calculated from linear extrapolation of air temperatures and precipitation at referenced stations with mean altitudinal gradients (Table1).

To describe atmospheric circulation patterns that influence regional precipitation regimes at seasonal time scales, we used monthly data on the frequency of synoptic patterns observed over southwestern Siberian Altai and central Tien Shan Mountains developed by Popova (*1972*), Narojniy and others (*1993*), Bugaev and others (*1957*) and Subbotina (*1995*) and partially presented in the Central Asia Data Base (CADB), which is completed and maintained by the authors at the University of Idaho. A brief description of synoptic pattern classifications over Siberia and Central Asia is presented in Aizen

and others (*2004, 2005*). The prevailing synoptic patterns associated with precipitation are listed in Table 2.

*Table 1. Gradient ranges established from monthly (m) or annual (a) station data: γ(T) °C/100m; γ(P), mm/100m is air temperature and precipitation gradients; H, is elevation in meters*

| Location | Station | $H_{station}$ | Drilling glacier | $H_{drill\ site}$ | $\gamma_m(P)$ | $\gamma_a(P)$ | $\gamma_m(T)$ | References |
|---|---|---|---|---|---|---|---|---|
| Siberian Altai | Kara-Turek | 2600 | Belucha | 4110 | 0.18 to 2.2 | | -0.06 to -0.46 | Aizen and others, 2005 |
| | Akkem | 2045 | 49°48'N, 86°32'E | 4110 | 0.18 to 2.2 | 7 | -0.06 to -0.46 | |
| Central Tien Shan | Tien Shan | 3614 | Inylchek 42°13'N, 80°12'E | 5200 | | 63 | -0.05 to -0.54 | Aizen and others, 1997; 2004 |
| South-East Tibet | Zuoqiupu Bomi Chayu Linzhi | 5200 2736 2328 2992 | Zuoqiupu 29°30'N, 97°00'E | 5795 | -6.7 to 12 | 31 to 34 | -0.05 to -0.56 | Current research |

*Table 2. Clustered average/extreme δ¹⁸O and d-excess values from accumulation layers formed by precipitation originated from central Asian (CA) and Oceanic moisture sources and their share in the total annual and seasonal accumulation layers. SP is prevailing synoptic pattern*

| SP | clusters | $\delta^{18}O$, ‰ | | | d-excess, ‰ | | | Share, % | | | | |
|---|---|---|---|---|---|---|---|---|---|---|---|---|
| | | max | min | Ave | max | min | ave | year | spr | summ | aut | wint |
| **Altai (17 years)** | | Total accumulation layer, mm | | | | | | 12591 | 3037 | 6752 | 1967 | 834 |
| | **average** | Annual accumulation layer, mm | | | | | | 690 | 133 | 376 | 129 | 52 |
| SWC | **CA** including E. Black&Caspian | -9.6 | -24.7 | -14.1 | 25.6 | 12.0 | 14.7 | 33 | 33 | 32 | 40 | 24 |
| | **Oceanic** | -8.1 | -19.7 | -13.3 | 12.0 | 1.1 | 8.1 | 67 | 67 | 68 | 60 | 76 |
| WC | Atlantic | -9.7 | -19.7 | -13.8 | 12.0 | 7.0 | 9.6 | 56 | 57 | 60 | 36 | 76 |
| UP, NWC StCyc | Arctic/ Pacific | -8.1 | -16.7 | -12.4 | 7.8 | 1.1 | 5.6 | 11 | 10 | 8 | 24 | |
| **Tien Shan (5 years)** | | Total accumulation layer, mm | | | | | | 5300 | 1670 | 2350 | 960 | 320 |
| | average | Annual accumulation layer, mm | | | | | | 1060 | 334 | 470 | 193 | 63 |
| SC | **CA** | -10.8 | -31.98 | -20.3 | 45.0 | 22.0 | 28.2 | 55 | 72 | 32 | 68 | 94 |
| WC | E. Mediterranean, Black Seas | -7.4 | -24.6 | -13.3 | 21.9 | 15.7 | 18.9 | 32 | 23 | 44 | 27 | 6 |
| | **Oceanic** | | | | | | | | | | | |
| IW | N.Atlantic | -7.0 | -16.9 | -10.5 | 15.6 | 9.3 | 13.0 | 13 | 5 | 24 | 5 | |

*Note: spr., summ, aut, wint are spring, summer, autumn, winter; **Altai:** SWC is South West Cyclone; WC is West Cyclones; UP is Ultra Polar intrusions; StCyc is stationary Cyclones; **Tien Shan:** WC is Western Cyclones; IW Influxes of air masses from west; SC are southern cyclones including South-Caspian, Murgab and Upper Amy Darya' cyclones*

**Climatic regime**

All study locations exhibit maximum temperature and precipitation during the summer months. Two of these, Tien Shan in central Asia and Altai in the Siberian mountains, are distinguished by a continental climate with significant annual air temperature variation, up to 20ºC at the Tien Shan and 16ºC at the Altai drilling sites (Fig. 3b). These glaciers store records of the advection of fresh water transferred from the Atlantic, Pacific, and Arctic Oceans (*Aizen and others, 2004; 2005*) (Fig. 2). The firn records from the Tien Shan and Altai glaciers can be directly associated with one of the world's largest internal water systems (i.e., Aral-Caspian and Tarim).

The third studied region is the Bomi glacial massif located in the Hengduan Range of southeastern Tibet, along the windward slope of the Southwest monsoon. Annual air temperature variation is significantly less (13ºC) in southeast Tibet than at the central Asian drilling sites (Fig. 3b). Under the influence of the monsoon, the heaviest amounts of precipitation occur at the Tibetan study location (Fig. 3a).

## MEASUREMENTS, PROCESSING AND ANALYSES
### Field sampling and measurements
The firn/ice cores, snow pits and fresh snow samples obtained during field seasons from 1998 to 2003 were collected using established sampling techniques for isotope-geochemical analysis (*Aizen and others, 2004; 2005; Kreutz and others, 2001; 2003*). Core dimensions and weight were measured, followed by detailed description of the physical stratigraphy using a light table and photographs of each core section. The seasonal layers in Tien Shan and Altai were differentiated from the others by their crystal structure (Fig. 4) (*Aizen and others, 2004, 2005*). Each drill run was photographed, packed into pre-cleaned plastic packets and shipped frozen from the drilling sites to the University of Idaho (UI) and University of Main (UM) where they are currently stored.

The drilling sites were identified as suitable locations for recovery of firn-ice cores and subsequent development of climatic records. Summer air temperatures (Fig. 3a), snow pit, and firn core temperatures (Fig. 7) and stratigraphy profiles (Fig. 4) revealed negligible snow melt and the absence of melt water percolation, which redistributes isotopic signals.

The stratigraphic profiles from the Tien Shan and Altai firn/ice cores

**Fig. 4.** *Snow/firn physical stratigraphy with seasonal and annual layer identification in the Siberian Altai 21 m snow/firn core recovered from the West Belukha plateau.*

show drier, colder depositional environments representing the cold recrystalization zones of glacier accumulation areas with less annual accumulation at lower altitudes compared to Southeast Tibet (Figs. 4, 5, 6). Temperature profiles show decreasing temperatures with depth, and although the temperature profile at the Southeast Tibetan site shows increasing temperatures in the first one meter before decreasing with depth, the entire profile is below 0ºC. Snow pit density ranges are similar at the central Asia (0.22 g cm$^{-3}$ at the surface to 0.49 g cm$^{-3}$ at 2 m snow depth) and at the Southeastern Tibet (0.21 – 0.55 g cm$^{-3}$), although at the last site density increases more rapidly within the first three meters (Fig. 3). A warmer, wetter depositional environment at the southeastern Tibet site with precipitation closer to 0ºC result in the distinctive feature of occasional thin (1-3 mm) wind/solar radiative crusts in the stratigraphic profiles (Fig. 4).
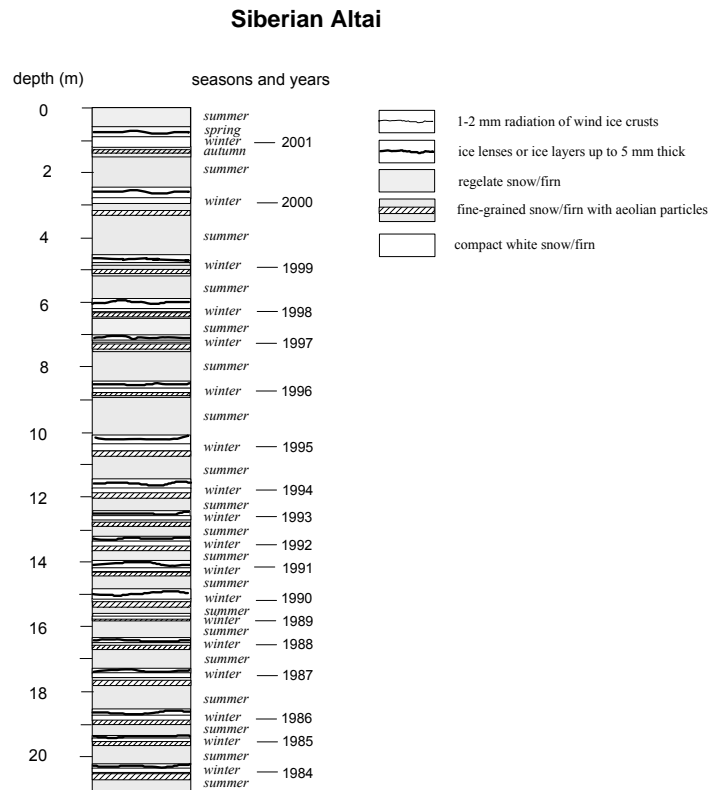
In the remote field locations, Grant Instruments and Campbell Scientific (Logan, UT) automated weather stations and data loggers were used to record hourly measurements of air and ice temperatures. An automatic snow depth gauge (KADEC-SNOW, KONA system) was installed on the Altai glacier drilling site in July 2001, with sensor detection of snow or open air by photo-diodes at an interval of 1 cm. Two daily measurements, one in the morning and one in the evening, recorded the snow surface level for two months.

**Stable isotope processing**

Each 3–5 cm of the upper part of the snow/firn core, as well as samples from five snow pits, and fresh snow, were analyzed for $\delta^{18}O$ and $\delta D$ in collaboration with the UI, UM, University of New Hampshire, and the National Institute of Polar Research in Tokyo. The analytical precision for measurements of oxygen and deuterium isotopic ratios was ±0.05 and ±0.5‰ respectively in each laboratory. The technique of snow/firn-core stable-isotope processing and analysis has been described by Kreutz and others (2001).
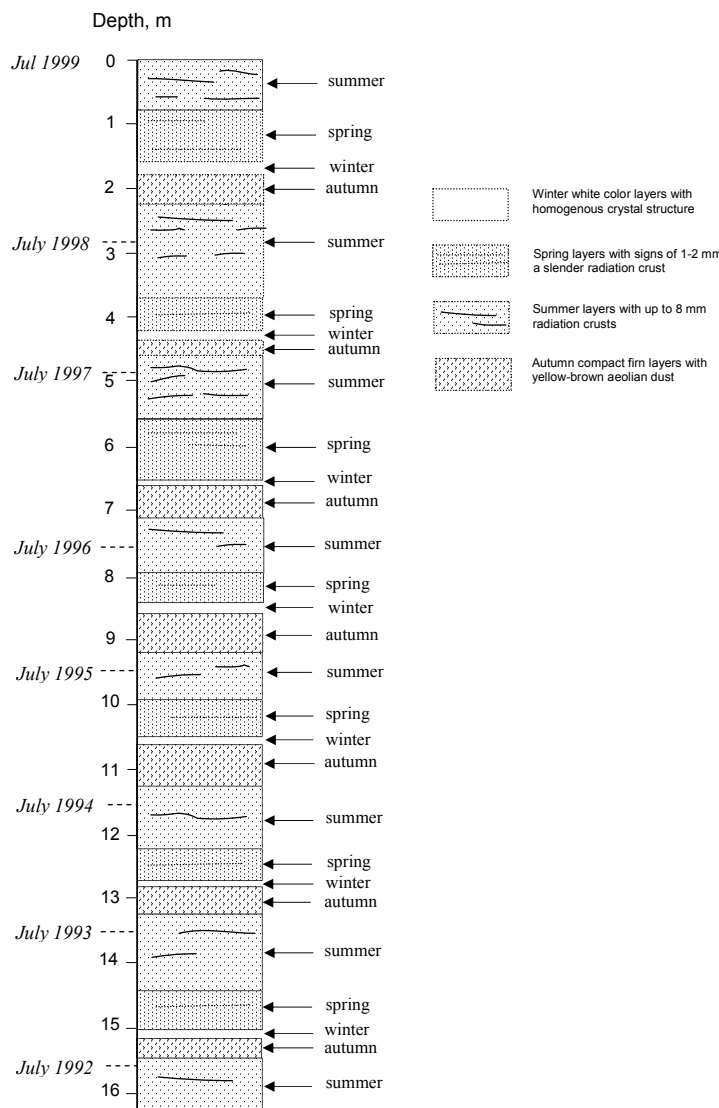
**DATA ANALYSIS TECHNIQUE**
**Ice core/snow pit dating**

Ice core dating was preliminarily assigned through counting of annual layers based on detailed inspection of the visible stratigraphy (Fig. 5). The established ice core chronology was further refined by counting annual layers in stable isotopes (Fig. 8), which show well preserved annual variation profiles (*Kreutz and others, 2001; Aizen and others, 2004; 2005*). The mean accumulation rate obtained from the shallow Altai ice cores agrees with the rate validated through tritium and ^{210}Pb records by Olivier and others (2003). Annual net accumulation at field sites amounted to 690 mm at the Belukha, 1060 mm at the Inilchek and 1960 mm at the Zuoqiupu drilling sites.

To determine the seasonal and monthly accumulation and corresponding seasonal and monthly isotope means, the normalization technique (Barlow and others, 1993; Shuman and others, 1995; Yao and others, 1999; Aizen and others, 2004) was applied. Annual accumulation at the drilling site was normalized by the



**Fig. 5** *Snow/firn physical stratigraphy with seasonal and annual layer identification in the Tien Shan 16 m firn/ice crevasse located at the edge of the Inilchek Glacier accumulation area;*

share/fraction of monthly/seasonal precipitation in annual total at the referenced station. To verify the

core chronology in the Altai ice core, we used the marker horizon of the Mt. Pinatubo volcanic eruption (June, 2001*).* The ice layers of volcanic origin have been deduced from acidity measurements along firn/ice cores (*Zielinski and others, 1996*). The sulfate peak measured at ice core is related to firn core layer of May-June 1991, corresponding to the Mt. Pinatubo eruption with monthly precision.

Calculated seasonal snow accumulation layers were differentiated by crystal structure and were identified by the presence of yellow-brown aeolian dust. Uncertainty in calculating seasonal accumulation using the normalization technique was less than ±10% of the seasonal accumulation rate obtained from the snow/firn core stratigraphic profile. Snow-firn stratigraphic profiles allowed proportioning the firn core layers at seasonal resolution, while monthly precipitation data from the closest meteorological stations detailed the firn core records with monthly resolution for spring, summer and autumn seasons. The thin winter layers were considered as the sum of accumulation for three months.

To evaluate the links between isotope/geochemical records in the firn core profile and synoptic pattern prevalence, we calibrated the measured isotope values in snow pit layers to corresponding dates of the observed prevailing synoptic pattern. The automatic daily measurements of surface level changes provide daily information on snow accumulation at the Altai drilling site during two months, enabling calibration of the isotope-geochemistry records in snow pits at event scale, with a standard error of 7.5 mm (*Aizen and others, 2005*).

Monthly snow accumulation values for 2000, calculated by the normalization technique agreed with corresponding values calculated using the event snow surface changes. The normalization techniques at the Tien Shan drilling site was validated through precipitation events at the Tien Shan station and corresponding accumulation layers in the snow pit stratigraphy (Fig. 6; *Aizen and others, 2004*).
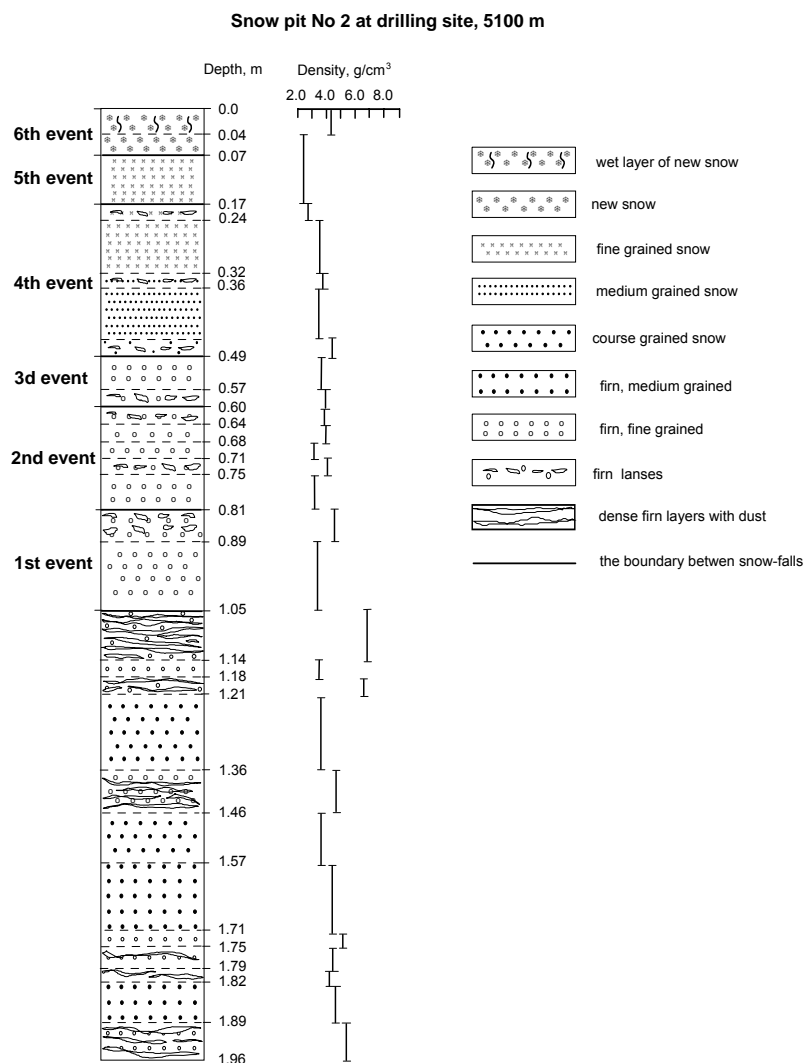


**Fig. 6.** *Snow stratigraphy, snow density and layers of six precipitation events in snow pit on the Inilchek Glacier (*Aizen and others, 2004*).*

## Clustering precipitation transferred from oceanic and central Asian moisture sources

To distinguish oceanic moisture from water vapor re-evaporated from internal basins and transferred to the high/middle latitudes of Asia, the $\delta^{18}O$ isotopic ratio and d-excess values from 524 samples from the Altai and 264 samples from the Tien Shan cores were clustered into two distinct datasets. The clustering

procedure was based on the K-means clustering analysis of splitting a set of data into two groups by maximizing between-cluster variation relative to within-cluster variation (Table 2).



**Fig. 7.** *Borehole temperature profiles and snow pit temperatures.*

To evaluate the link between stable isotope concentrations in the firn core profile and atmospheric circulation dynamics, we matched the measured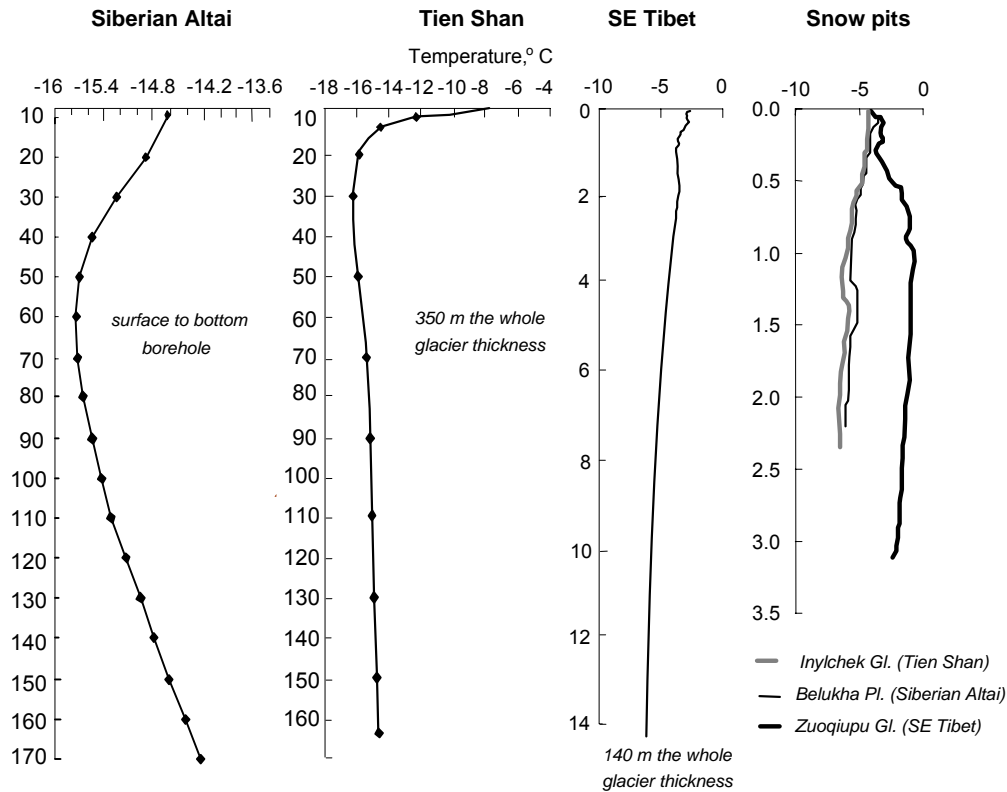 $\delta^{18}O$ and d-excess values in snow pit layers to corresponding precipitation events observed at the meteorological stations. The snow accumulation event values in the snow pit were calculated using a normalization technique. The $\delta^{18}O$ values and d-excess mean in snow layers during precipitation events were related to the synoptic patterns of associated precipitation (*Aizen and others, 2004; 2005*). Analysis of synoptic processes prevailing during precipitation events over West Siberia and Central Asia are in accordance with results from the K-means clustering analysis, with about a 15% deviation (i.e., the accumulation where the stable isotope distribution was not in accordance with developed clustering amounted to 929 mm in total Altai accumulation of 12,591 mm). The main uncertainty occurred during winter months when several insignificant precipitation events with both oceanic and inter-land moisture sources were associated with the same snow accumulation layer.

## CONTRIBUTION OF OCEANIC AND CENTRAL ASIAN MOISTURE SOURCES
### Clusters
The revealed clusters for Altai ice core records are: Oceanic sources with d-excess less than 12‰, and the Aral–Caspian closed drainage basin sources with d-excess exceeding 12‰ (up to 25.6‰). Oceanic source is differentiated from Atlantic moisture source with d-excess ranging from 7.0‰ to 12‰. Moisture of Arctic and Pacific origin is associated with the lowest d-excess levels (< 7.8‰). The main synoptic pattern that brings moisture to the Siberian Altai is the *western cyclones* pattern from the Atlantic Ocean. Strong depletion in $\delta^{18}O$ and in d-excess records is associated with synoptic patterns of *North Western and Ultra-Polar* cyclones that bring moisture from the Arctic Ocean. Increased

development of *stationary cyclones* is associated with $\delta^{18}O$ enrichment and d-excess depletion. High d-excess values are associated with precipitation carried by *southwestern cyclones* and are a result of re-evaporating water vapor from the internal Aral-Caspian basin.

The revealed clusters for Tien Shan ice core records are: re-cycled precipitation has the highest d-excess values ranged from 15.6 to 45‰, re-evaporated precipitation originating over the Aral-Caspian basin and brought by *southern cyclones* has d-excess > 22.0‰, and precipitation re-evaporated over the Eastern Mediterranean and Black Seas has records with 15.6< d-excess <22.0‰ values. The *western influxes from the Northern Atlantic* bring precipitation with low d-excess values ranged from 9 to 16 ‰.



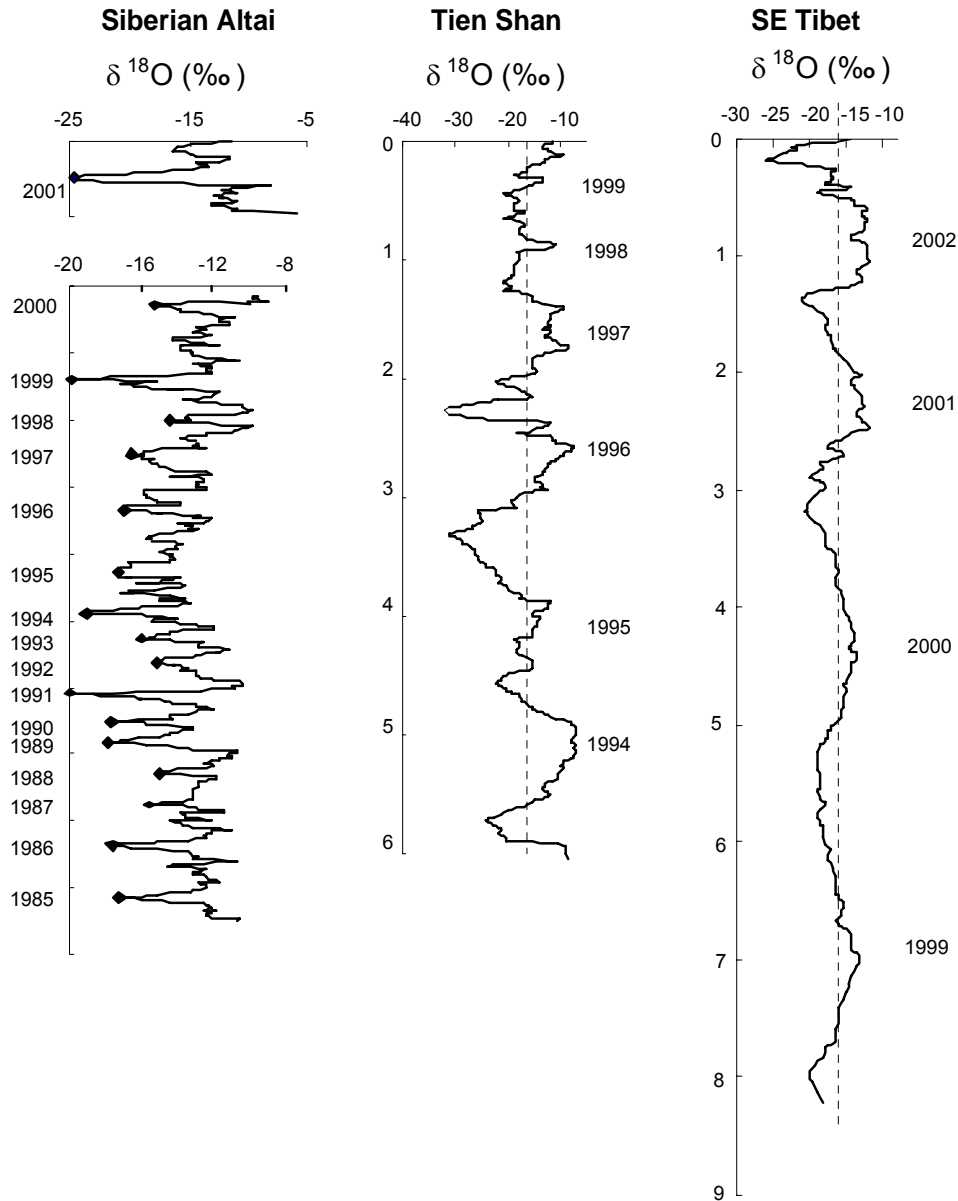**Fig. 5.** *Iso8opic composition, $\delta^{18}O$ in snow/firn cores*

Most enriched $\delta^{18}O$ snow accumulation layers of -7.0‰ are typical during domination of this synoptic mode. Contributions of precipitation originating from external and internal moisture sources to mean annual/seasonal accumulation at the Altai and Tien Shan locations were estimated through the developed clustering (Table 2).

13

**Altai accumulation**

The largest share (67%) of total snow/firn accumulation corresponds to precipitation transferred by *Western, Northwestern, Stationary Cyclones, and Ultra Polar intrusions* from oceanic moisture sources (Table 3). Precipitation over the Siberian Altai is mainly marine in origin during all seasons, with the oceanic share almost invariable, ranging from 76% in winter to 60% in autumn accumulation. Moisture evaporated over the Atlantic Ocean comprises more than half of the annual accumulation (56%). Precipitation transferred from Arctic Ocean or an eastern moisture source, with the lowest d–excess levels, comprises 11% of the annual accumulation with autumn maximum (24%) and summer minimum (8%).
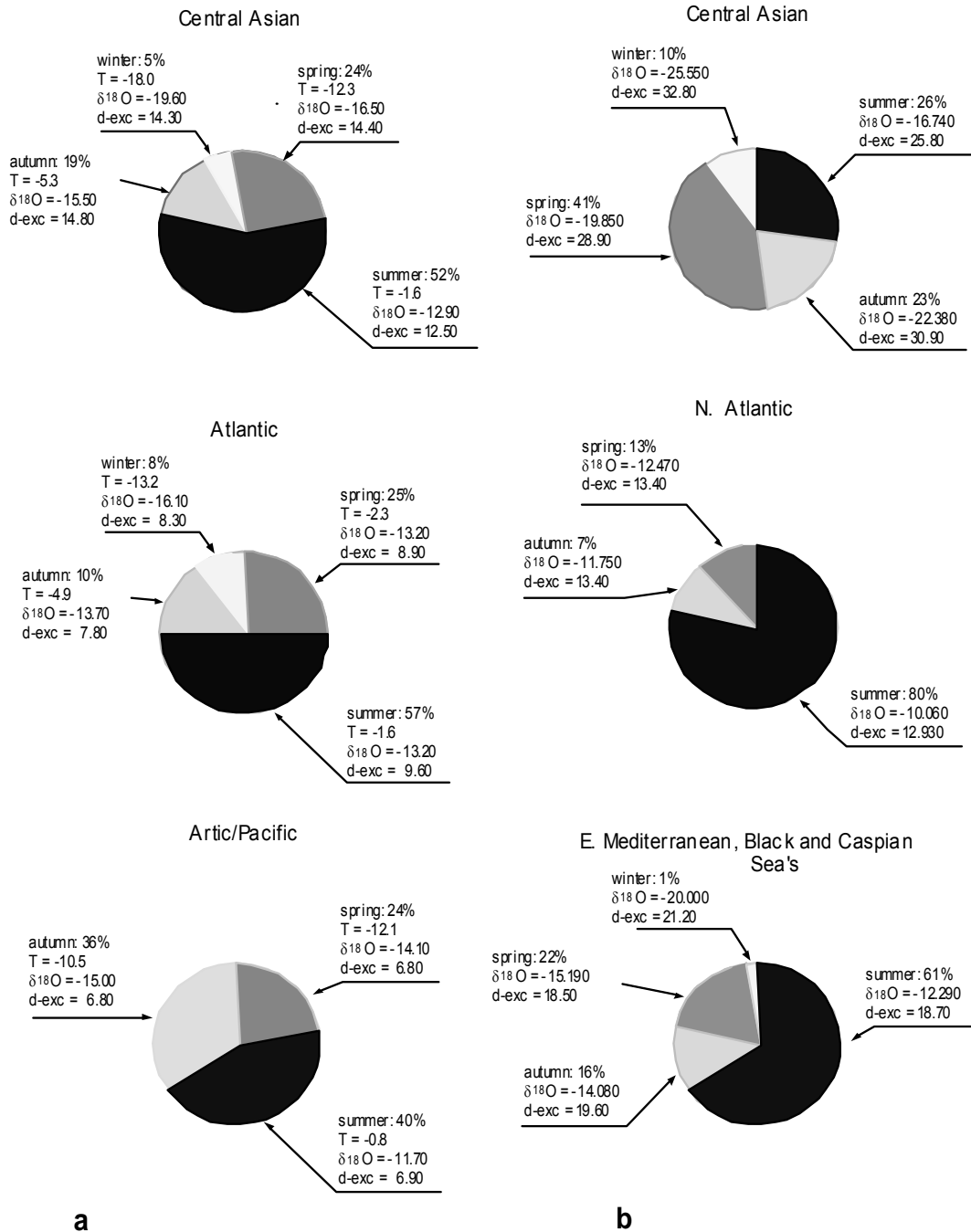


Central Asian

winter: 5%
T = -18.0
$\delta^{18}O$ = -19.60
d-exc = 14.30

spring: 24%
T = -12.3
$\delta^{18}O$ = -16.50
d-exc = 14.40

autumn: 19%
T = -5.3
$\delta^{18}O$ = -15.50
d-exc = 14.80

summer: 52%
T = -1.6
$\delta^{18}O$ = -12.90
d-exc = 12.50

Central Asian

winter: 10%
$\delta^{18}O$ = -25.550
d-exc = 32.80

summer: 26%
$\delta^{18}O$ = -16.740
d-exc = 25.80

spring: 41%
$\delta^{18}O$ = -19.850
d-exc = 28.90

autumn: 23%
$\delta^{18}O$ = -22.380
d-exc = 30.90

Atlantic

winter: 8%
T = -13.2
$\delta^{18}O$ = -16.10
d-exc = 8.30

spring: 25%
T = -2.3
$\delta^{18}O$ = -13.20
d-exc = 8.90

autumn: 10%
T = -4.9
$\delta^{18}O$ = -13.70
d-exc = 7.80

summer: 57%
T = -1.6
$\delta^{18}O$ = -13.20
d-exc = 9.60

N. Atlantic

spring: 13%
$\delta^{18}O$ = -12.470
d-exc = 13.40

autumn: 7%
$\delta^{18}O$ = -11.750
d-exc = 13.40

summer: 80%
$\delta^{18}O$ = -10.060
d-exc = 12.930

Artic/Pacific

spring: 24%
T = -12.1
$\delta^{18}O$ = -14.10
d-exc = 6.80

autumn: 36%
T = -10.5
$\delta^{18}O$ = -15.00
d-exc = 6.80

summer: 40%
T = -0.8
$\delta^{18}O$ = -11.70
d-exc = 6.90

E. Mediterranean, Black and Caspian Sea's

winter: 1%
$\delta^{18}O$ = -20.000
d-exc = 21.20

spring: 22%
$\delta^{18}O$ = -15.190
d-exc = 18.50

autumn: 16%
$\delta^{18}O$ = -14.080
d-exc = 19.60

summer: 61%
$\delta^{18}O$ = -12.290
d-exc = 18.70

**a**

**b**

The remaining 34% corresponds to precipitation transferred by *Southwest Cyclones* and recycled over internal moisture sources, with the largest share (40%) occurring in autumn. The smallest share of recycled precipitation (24%) transferred from internal moisture sources to the Altai glaciers was observed in winter, when the Siberian High is strongest, blocking any intrusion of air masses, and conditions for inland evaporation and local convection are weakest because of low continental heating.
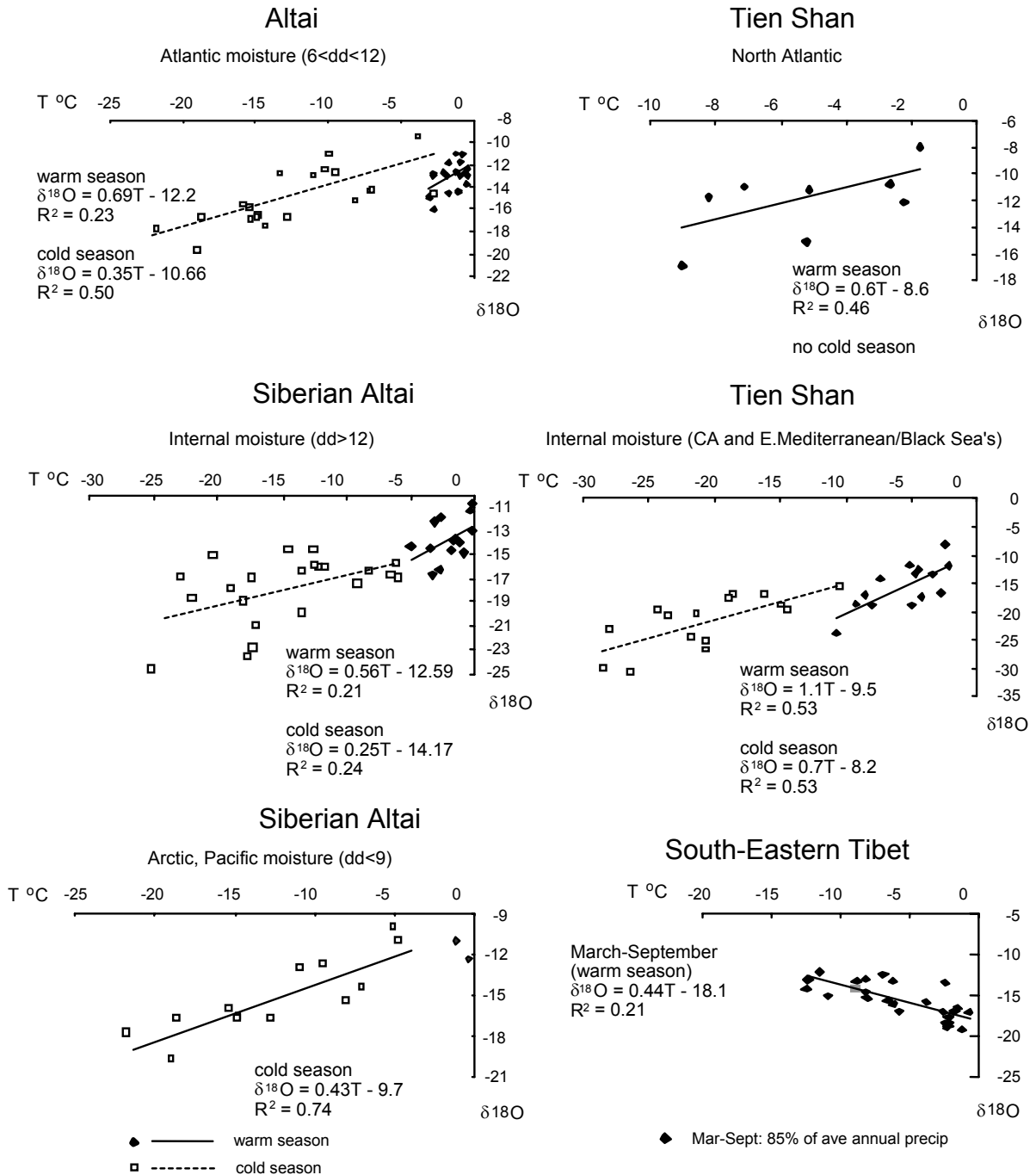


**Altai** — Atlantic moisture (6<dd<12)

warm season
$\delta^{18}O = 0.69T - 12.2$
$R^2 = 0.23$

cold season
$\delta^{18}O = 0.35T - 10.66$
$R^2 = 0.50$

**Tien Shan** — North Atlantic

warm season
$\delta^{18}O = 0.6T - 8.6$
$R^2 = 0.46$

no cold season

**Siberian Altai** — Internal moisture (dd>12)

warm season
$\delta^{18}O = 0.56T - 12.59$
$R^2 = 0.21$

cold season
$\delta^{18}O = 0.25T - 14.17$
$R^2 = 0.24$

**Tien Shan** — Internal moisture (CA and E.Mediterranean/Black Sea's)

warm season
$\delta^{18}O = 1.1T - 9.5$
$R^2 = 0.53$

cold season
$\delta^{18}O = 0.7T - 8.2$
$R^2 = 0.53$

**Siberian Altai** — Arctic, Pacific moisture (dd<9)

cold season
$\delta^{18}O = 0.43T - 9.7$
$R^2 = 0.74$

warm season
cold season

**South-Eastern Tibet**

March-September
(warm season)
$\delta^{18}O = 0.44T - 18.1$
$R^2 = 0.21$

Mar-Sept: 85% of ave annual precip

15

Summer is the main season of accumulation, i.e., both from external and internal moisture sources (Fig. 9). The Atlantic moisture as well as recycled moisture over central Asia was brought to the Siberian Altai year-round. From autumn to spring, $\delta^{18}O$ records associated with inter-land moisture sources are more depleted than $\delta^{18}O$ records related to Atlantic moisture sources because of lower air temperatures over the continent than over the ocean. Summer mean isotope records are almost the same. The mean values of $\delta^{18}O$ from summer accumulation layers with Arctic/eastern originated precipitation sources are the most enriched among the three considered clusters, reaching -11.7‰. The highest $\delta^{18}O$ values may be associated with the highest air temperature during precipitation and/or nearby water vapor formation, e.g., Arctic/ Pacific Ocean or local summer convection.



Count = 524
Mean = -13.7‰
Stdev = 2.1‰
Minimum = -24.7‰
Median = -13.3‰
Maximum = -8.1‰



Count = 264
Mean = -16.4‰
Stdev = 5.6‰
Minimum = -32.0‰
Median = -15.8‰
Maximum = -7.0‰



Count = 144
Mean = -16.3‰
Stdev = 2.6‰
Minimum = -26.0‰
Median = -16.3‰
Maximum = -11.8‰

**Fig. 10.** *$\delta^{18}O$(‰) data description and basic statistics of records from 4115 m of the  Belukha Plateau, Siberian Altai (1984-2001); 5200 m Inilchek Glacier, Tien Shan (1991-1998) and 5795 m of the Bomi glaciation, Tibet (1998-2001).*

**Tien Shan accumulation**

Central Asia receives most of its moisture from the west and its interiors are heavily depend upon the intensity of zonal water vapor transport. *Influxes of air masses from the west* are one of the main synoptic modes in the central Tien Shan, and these air masses bring 13% of marine-derived precipitation from the North Atlantic Ocean, with the highest annual values of $\delta^{18}O$ and the most depleted d-excess means. The percentage of summer moisture from North Atlantic reached 24% of total summer mean (Table 2).

*Western cyclones* originating over the eastern Mediterranean and Black Seas brought more significant precipitation to the central Tien Shan, comprising up to 32% of the annual and reaching 44% during summer. Because of very hot summers, the precipitated water in central Asia is recycled several times inside the Aral-Caspian closed drainage basin and is even transported to the Arctic basin. Maximum contribution to central Tien Shan accumulation is associated with recycled moisture (up to 87%) including 55% from Aral-Caspian and 32% from the eastern Mediterranean and Black Seas. During spring the maximum contribution occurred due to re-cycled moisture from Central Asia, reaching 72%, because warming of the inner continental regions occurs faster than in the coastal regions, increasing inland evaporation. During winter all of central Asia is blocked by the Siberian High. The minimal winter
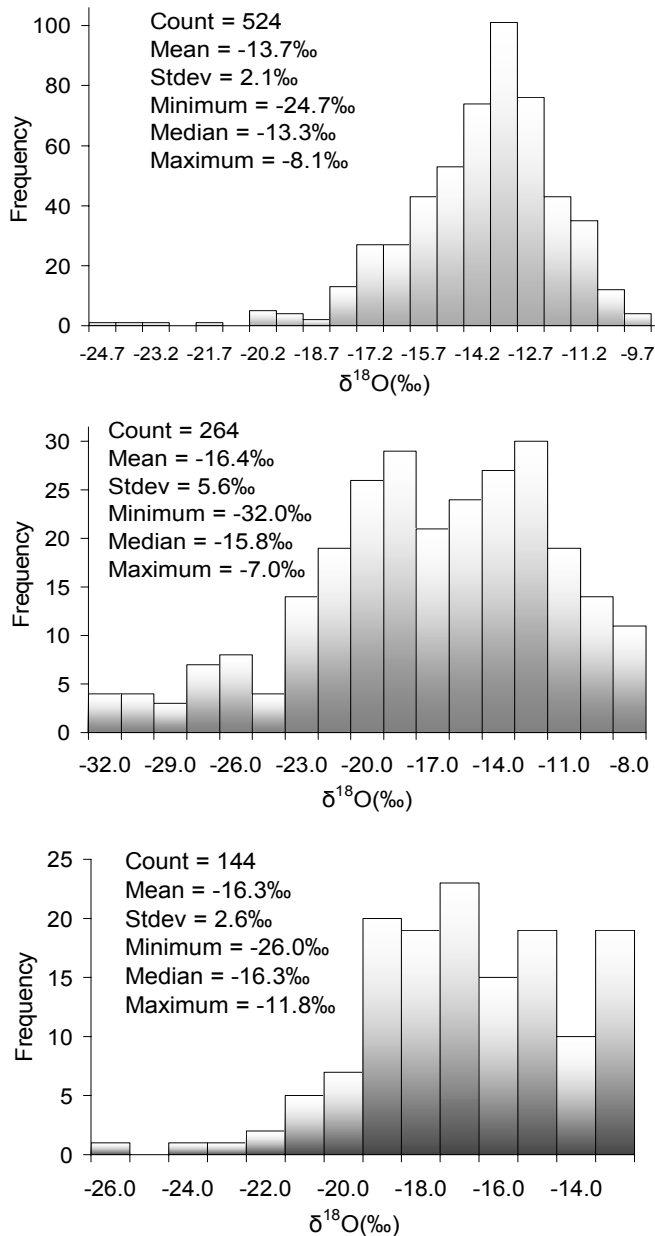
16

precipitation mainly originated over central Asia (up to 94%), with the highest d-excess values (maximum up to 45‰) (Table 2).

Summer is the main season of accumulation, as well as at the Altai location (Fig. 6), reaching 80% in North Atlantic originated precipitation. There are no records with low d-excess values (N. Atlantic) in accumulation layers related to winter months, while re-cycled moisture over Central Asia was brought to the central Tien Shan year-round.

*Table 3. Linear trends (β) of (A) monthly precipitation and air temperature at the Akkem station; (B) isotope and geochemistry records obtained from Siberian Altai ice-core and corresponding long-term monthly climatic variables for the period from 1984 to 2001; Bold font corresponds to statistically significant linear trend at 10%*

(**A**)

| | JAN | FEB | MAR | APR | MAY | JUN | JUL | AUG | SEP | OCT | NOV | DEC | YEAR |
|---|---|---|---|---|---|---|---|---|---|---|---|---|---|
| Precipitation | | | | | | | | | | | | | |
| $\beta$, yr$^{-1}$ | 0.45 | 0.52 | 0.53 | 0.20 | -0.01 | 0.02 | 0.01 | 0.02 | 0.04 | 0.03 | -0.11 | 0.10 | 0.03 |
| $\sigma_\beta$ | 0.32 | 0.31 | 0.21 | 0.05 | 0.06 | 0.04 | 0.05 | 0.07 | 0.07 | 0.07 | 0.17 | 0.26 | 0.02 |
| $r^2$ | 0.11 | 0.14 | 0.28 | 0.45 | 0.00 | 0.01 | 0.00 | 0.01 | 0.02 | 0.01 | 0.02 | 0.01 | 0.13 |
| F | 2.04 | 2.69 | **6.58** | **13.69** | 0.01 | 0.26 | 0.06 | 0.12 | 0.31 | 0.18 | 0.43 | 0.15 | 2.56 |
| Air Temperature | | | | | | | | | | | | | |
| $\beta$, yr$^{-1}$ | -0.23 | 1.30 | 0.77 | 0.92 | 1.81 | 3.24 | 3.22 | 3.94 | 0.62 | 0.71 | 0.47 | 0.00 | 4.17 |
| $\sigma_\beta$ | 0.49 | 0.39 | 0.45 | 0.63 | 0.67 | 0.77 | 1.32 | 1.09 | 0.62 | 0.46 | 0.42 | 0.48 | 0.98 |
| $r^2$ | 0.01 | 0.40 | 0.15 | 0.11 | 0.30 | 0.51 | 0.26 | 0.43 | 0.06 | 0.12 | 0.07 | 0.00 | 0.52 |
| F | 0.23 | **11.35** | 2.93 | 2.14 | **7.24** | **17.85** | **5.97** | **13.03** | 1.02 | 2.36 | 1.23 | 0.00 | **18.15** |

(**B**)

| | P, | T C | Isotope, ‰ | | Dust number/mL | particles | | Major ions, ppb | | | SP, days | |
|---|---|---|---|---|---|---|---|---|---|---|---|---|
| | mm | | $\delta^{18}$O | d-excess | total | 4.00-5.04μm | Volume, ppb | Cl$^-$ | Na$^+$ | Ka$^+$ | NWC | SWC |
| $\beta$, record$^{-1}$ | 0.35 | 0.007 | 0.002 | -0.0015 | 0.0001 | -0.02 | 0.0001 | 0.25 | 0.55 | 0.59 | 0.0.9 | -0.06 |
| $\sigma_\beta$ | 0.004 | 0.001 | 0.005 | 0.0012 | 0.0001 | 0.006 | 0.0000 | 0.1 | 0.13 | 0.29 | 0.016 | 0.09 |
| $r^2$ | 0.004 | 0.001 | 0.0003 | 0.0056 | 0.0087 | 0.081 | 0.06 | 0.029 | 0.08 | 0.12 | 0.006 | 0.02 |
| F | 0.93 | 0.42 | 0.1463 | **2.9** | 1.73 | **17.34** | **12.02** | **5.95** | **17.59** | **27.52** | 1.12 | 0.83 |
| n | 217 | 217 | 524 | 524 | 199 | 199 | 199 | 199 | 199 | 199 | 204 | 204 |

*Note: P and T is monthly annual precipitation and air temperatures SP is frequency of synoptic patterns; $\sigma_\beta$ is standard error values for slope coefficient; $r^2$ is coefficient of determination; F is F statistics; n is number of records; n is number of record; NWC and SWC is monthly frequency of north-western and south western cyclone.*

## STABLE ISOTOPE-AIR TEMPERATURE RELATIONSHIP

Local isotope-temperature relationships were calibrated using the seasonal air temperatures and prevailing atmospheric circulation pattern. The Altai and Tien Shan ice core records of oxygen isotopic ratios and d-excess clustered according to moisture origin (Table 2) and differentiated with monthly resolution were related to corresponded monthly air temperature (Fig. 9), which was linearly extrapolated to the drilling sites.

Transfer function slopes (for Tien Shan and Altai) and intercept (for Altai) for warm season Atlantic moisture (Fig. 9) are similar to the $\delta^{18}O/T$ relationship ($\delta^{18}O=0.69T-13.6$) found by Dansgaard (*1964*) for North Atlantic precipitation.

The core data from the mountain systems with continental climate features exhibit positive regression line slopes, with more depleted precipitation occurring during the coldest winter temperatures. More shallow regression line slopes (0.69-0.35) are present for the Altai core record (Fig. 9) compared to regression line slopes (1.1-0.6) for the Tien Shan record. These differences relate to varying amounts of precipitation, moisture source regions, as well as differing temperature regimes (Fig. 3). Altai raw data histogram shows lower frequency of depleted accumulation than Tien Shan, which is associated with minimal cold season precipitation at the Altai study site (Fig. 10). The highest positive slopes are associated with internal moisture, possibly due to low inter-land humidity during evaporation and quicker processes of isotope depletion. The maximum slope is typical for the Inilchek summer accumulation formed by precipitation from internal moisture sources.

Glacier accumulation regions with marine climates are distinguished by a lowering of the slope, with negative regression line slopes typical for southern periphery monsoon regions. The Southeastern Tibet firn core isotope data was examined for months with the greatest amount of precipitation (March-September) producing isotope/air-temperature relationships with slopes of -0.44. Negative regression line slopes (Fig. 9) are associated with heavy amounts of depleted moisture arriving during periods of maximum precipitation (Mar-Sept) and warmest annual average temperatures. This opposite seasonal relationship of isotopic records has been previously observed at sub-tropical ice core locations by Thompson and others (2003), Qin and others (2002), as well as from isotopic records of precipitation from Southeast Asia (Araguás-Araguás and others, 1998).

**VARIABILITY IN THE ALTAI ICE CORE RECORDS**

To analyze the ability of ice core records to represent the climatic and atmospheric dynamic changes, linear trends, standard errors, coefficients of determination, and F-tests were calculated. Estimations were based on monthly means of isotope, geochemistry and dust particles data obtained from Altai ice core records for seventeen years (Table 3). Verification of the obtained trends occurred through long-term monthly climatic and synoptic data for the corresponding period. Linear trends for climatic variables (air temperatures and precipitation) were calculated for the period from 1984 to 2001. During this time, we found statistically significant increases in precipitation in March and April, and air temperatures in February, May, June, July and August (Table 3A). However, stable isotope records of $\delta^{18}O$ reflecting the air temperature variability did not show a trend for the considered period of years (Table 3B).

The d-excess records from the Altai ice core (Table 3B) show a negative trend for the period from 1984 to 2001. Deuterium excess is a parameter reflecting re-evaporation at land surfaces and/or mixing along air mass trajectories (*Merlivat and Jouzel, 1979*). The decreasing d-excess values from 1984 on -0.8‰ were probably caused by a changing source of moisture, e.g., by decreasing the share of re-evaporated precipitation or increasing the share of oceanic moisture (e.g., Atlantic/Arctic/eastern originated precipitation). Furthermore, decreased volume and concentration of dust particles (with sizes over 1.00 μm) and increased content of marine originated ions of sodium and chloride also verified the weakening of Central Asian re-evaporated precipitation in the Altai. There was also the tendency of positive trends (not statistically significant) in frequency of northwestern cyclones (Table 5b), which brought Atlantic moisture to the Altai. At the same time there was a tendency for decreasing frequency of synoptic patterns that brought moisture as well as dust particles from central Asia, i.e., South-western cyclones.

**FINDINGS**

The technique of coupling synoptic climatology and meteorological data with $\delta^{18}O$ and d-excess in firn core records was implemented to determine climate-related signals and to identify the origin of moisture. The firn core records were calibrated at event scale and validated using the monthly meteorological data

18

with 15% uncertainty. The method is applicable to reconstruct the climatic and atmospheric circulation dynamics over past centuries from surface-to-bottom deep ice cores recovered from the Belukha firn plateau and the Inilchek glacier. The clusters in $\delta^{18}O$ and d-excess records in the Altai and Tien Shan firn/ice cores revealed that the precipitation is oceanic in origin and re-cycled moisture from the Aral–Caspian closed drainage basin.

Two-thirds of the Altai accumulation is formed from oceanic precipitation for the period from 1984 to 2001; the rest of the precipitation is re-cycled over Aral-Caspian sources. More than half of the accumulation has an Atlantic Ocean origin, and precipitation from the Arctic and Pacific Oceans contributed about 11%. The inter-land moisture sources contributed the remaining 33% of annual Altai precipitation. The re-cycled annual amount of Tien Shan accumulation reached up to 87% of total, with the highest d-excess values. Precipitation, which is re-cycled from the Aral-Caspian basin contributed 55% and Mediterranean and Black seas produced about 30% to the Tien Shan mean annual accumulation. Only 13% of annual snow accumulation with low d-excess and most enriched $\delta^{18}O$ values is brought from the North Atlantic. However, from 1984 to 2001, there is tendency on the decreasing d-excess values in Altai ice core records that is in accordance with the decreasing dust content in corresponding ice core layers and the strengthening of synoptic patterns that brought precipitation of the Atlantic origin.

The ice-core data from the mountain systems with continental climate features exhibit positive regression line slopes in isotope/air-temperature annual/seasonal relationships, with a shallower slope for the Altai compared to the Tien Shan records. Glacier accumulation regions with marine climate are distinguished by a lowering of the slopes so that the negative regression line slopes are typical for southern periphery monsoon regions. Signs in regression line slopes for the northern periphery of the Asian mountain system as well for Southeast Tibet are comparable with results of Araguas-Araguas and others (*1998*) for Asia precipitation.


**PART II. STABLE-ISOTOPE and TIME SERIES from <u>PAMIR</u> FIRN CORE COMPARED with TIEN SHAN and ALTAI RECORDS**

**Overview**

<u>The proposed Pamir ice core, if it will be drilled, will be the deepest non-polar ice core record ever recovered</u>.

In July-August 2005 the project team accomplished first filed reconnaissance in Central Pamir to check logistics, recover several shallow snow-firn cores and establish an automatic weather station to collect meteorological data over the year period. Measurements of ice flow velocity and snow ablation accumulation rate were processed during 10 days period that gave us estimations for further research in this area. The Fedchenko Glacier in Central Pamir is the largest alpine glacier at mid- low- latitudes has thickest ice body reached 1000 m at low glacier accumulation area and may contain longest climatic records from the mid- low- latitudes extending back over 100,000 years. There are also several accumulation zones in the Pamir mountains located over 5500 m with ice thicknesses greater than 500 m. These areas are suitable for the recovery and development of ice core climatic and environmental records. In addition, the Pamir long-term meteorological, synoptic, aerosol, and dust storm records provide an ideal platform for ice-core data calibration, validation and interpretation.

**First results**
**Stable isotopes and deuterium exces**
The main controls affecting the stable-isotope are air temperature, air humidity, air mass trajectories and source regions. The mean $\delta^{18}O$ ratio from the Pamir core of $-17.7‰$ is the most depleted among other isotope records obtained from central Asia (Fig. 19).

Fig. 19 Means and seasonal amplitude of $\delta^{18}O$ and d-excess from the central Asian ice cores
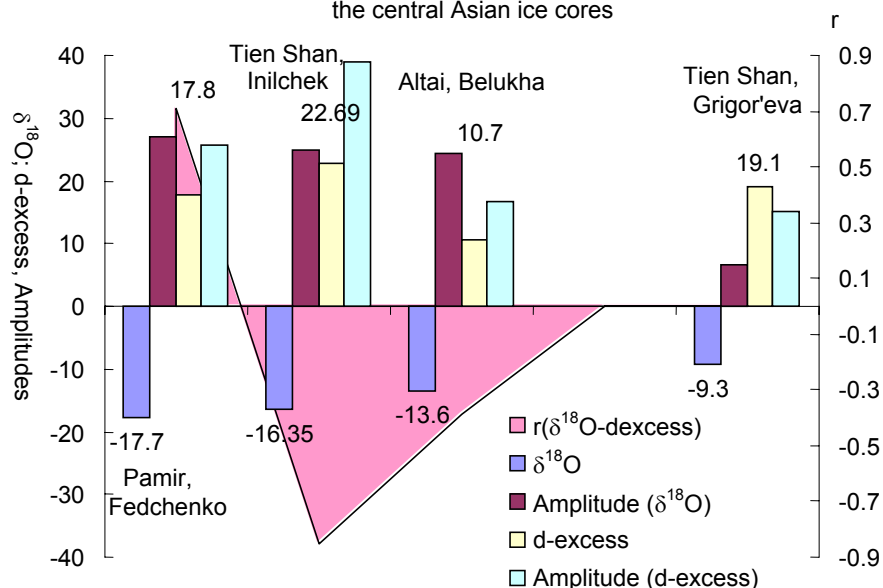
The analytical precision for measurements of oxygen and deuterium isotope ratio was ±0.05‰ and ±0.5‰ respectively. Analytic uncertainty in d-excess was 0.52‰, $\delta^{18}O$ ratios reflected a continental climate with the highest range between absolute maximum and minimum values of 24.6‰ (Fig. 19). Proportionally high cold season (maximum from November to April, Fig. 20) precipitation amounts at the Pamir compared to Tien Shan and Altai results in the lowest mean isotope ratio (−17.7‰).



Fig. 20 Monthly distribution of air temperature (TC), precipitation (P) and relative humidity (Rel Hum). Abramova Gl, Pamir
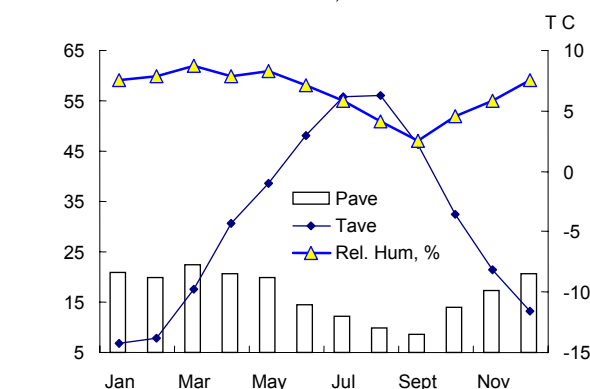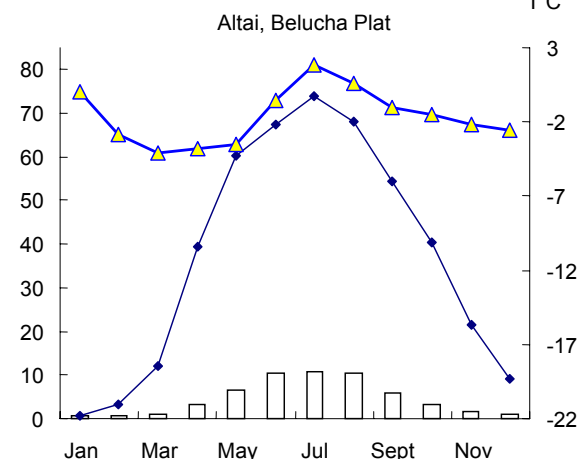
For example, 24% of cold season precipitation, with -16‰ of $\delta^{18}O$ low means during the cold season (Fig. 21), resulted in 2‰ depletion of the annual mean, while 60% of precipitation in the cold season at the Pamir, with -23‰ of $\delta^{18}O$ mean, resulted in 6‰ depletion.The distribution in $\delta^{18}O$ and $\delta D$ records from the Pamir snow/firn core shows well-preserved seasonal variations (Fig.22).

Seasonal deuterium excess and $\delta^{18}O$ variation from the Pamir firn core records differs from the other cores (Fig. 22) with both maximum in summer season and both minimum in winter. Only, a firn core from Tsast Ula ice cap, Mongolia, displays similar seasonal levels of d-excess and $\delta^{18}O$ (*Schotter and others, 1996*).

f, % Fig. 21. Probable (f, %) distribtion of $\delta^{18}O$ firn core records
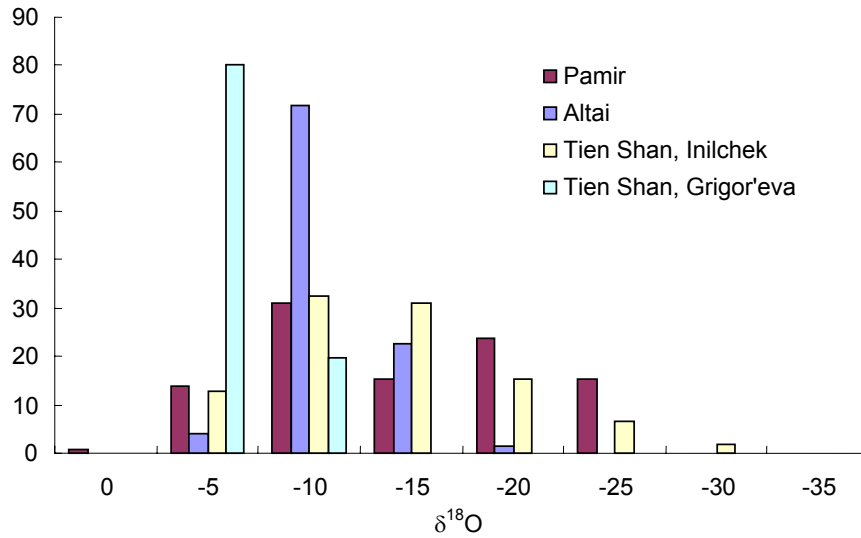
A firn/ice cores drilled in the Tien Shan, Inilchek as well as in the Altai exhibit inverted seasonal d-excess and $\delta^{18}O$ variability, i.e., lowest d-excess and highest $\delta^{18}O$ values correspond to the summer season with maximum precipitation and air temperatures. Winter maximum precipitation and strong summer evaporation on the Pamir could cause this different distribution (Fig. 22). Low humidity during warm season causes the effect of partial re-evaporation of snowflakes below clouds and sublimation from snow surfaces on the firn core records. Seasonal fluctuations of the $\delta^{18}O$ and d-excess relationship may provide insights into changes in the large scale atmospheric circulation pattern variability. During spring/winter season, when maximum precipitation is observed, the d-excess records are ranging from 8‰ to 11‰ (Fig. 22), with about the same intercept as for the GMWL. Western air masses from Atlantic bring precipitation to the Pamir. For summer/autumn seasons, d-excess increased up to 28.5‰ (Fig. 22) and reflect complicated sources of precipitation, e. g., the air masses originated over warm oceanic waters (Indian or/and south Atlantic oceans) and modification of air masses during passage over relatively warm continental waters.
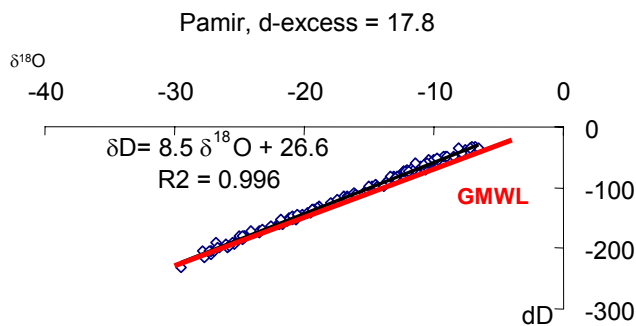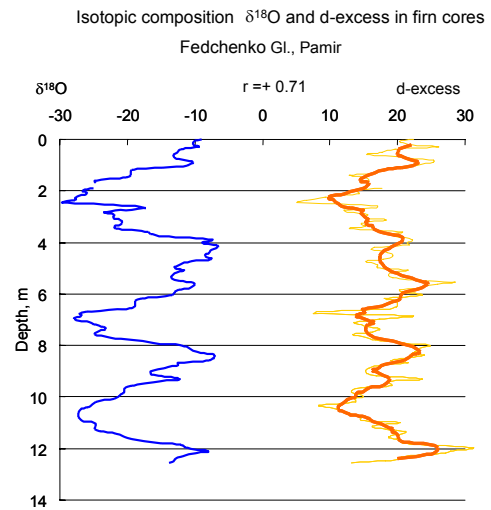
*Fig. 22.*



Isotopic composition $\delta^{18}O$ and d-excess in firn cores
Fedchenko Gl., Pamir



Pamir, d-excess = 17.8

$\delta D= 8.5 \, \delta^{18}O + 26.6$
$R2 = 0.996$

GMWL

*Fig. 23. Deuterium (δD) and oxygen ($\delta^{18}O$) isotope relationship*

21

The amount of d-excess is dependent on sea surface temperatures during evaporation. The long-term mean and seasonal amplitude of d-excess in the Pamir snow/firn core records (17.8‰, Fig. 19, 24) is between the Tien Shan and Altai firn core records of 23‰ to 10.7‰. The $\delta^{18}O$-$\delta D$ relationship in the snow/firn core from the Fedchenko Gl. (Fig 23) has a similar slope (i.e., 8.5) to the co-variance as that of the GMWL (i.e., 8), indicating the same initial relationship of fractionation factors, and points to the absence of strong melt and percolation in the snow/firn core. Deuterium excess is a parameter reflecting re-evaporation at land surfaces and/or mixing along air mass trajectories. A smaller or larger intercept in the local relationship, from the snow/firn core, fresh snow, snow pit and precipitation, compared with the GMWL (i.e, 10) reflects different kinetic evaporation effects on the transferred water vapor, e.g. initial water vapor was more quickly or slowly evaporated under non-equilibrium conditions (*Kendall and McDonnell, 1998*).

*Fig. 24.* Probable (f, %) distribution of $\delta^{18}O$ in firn core records
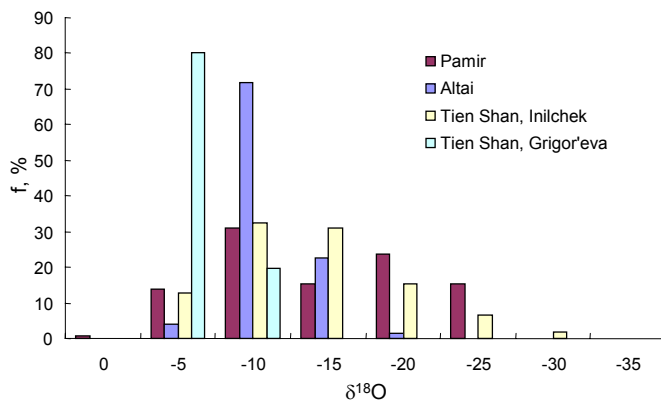
**Major and REE Concentrations in the Pamir firn core**

The vast arid and semi-arid regions of central Asia, Mongolia, Northern and Eastern China are the world's second largest source of atmospheric mineral dust. Spacious deserts of CA (e.g., Kara-Kum, Kyzyl-Kum, Muyun-Kum and Bet-Paqdala, Takla-Mahan) cover large areas from Mangishlak Peninsula to Balkhash Lake, to the north from the Kopet Dag, Pamir and Tien Shan mountains. Drying up of the Aral Sea affected large regions thousands of kilometers from Central Asia. Due to poor irrigation practices, by 1999 the width of dried sea bed reached 120 km, having a total dry area of about 40,300 km². The sea bed has become the world's sandy-solonchak desert, emitting vast amounts of salt and dust into the atmosphere. Major and REE (Fig. 25) elements concentration (average, maximum, background) from the Fedchenko (Pamir) firn core is ~1 magnitude (20 times) lower than a concentration from the Inilchek, Tien Shan where close location of Tackla-Mahan desert with foehn intensive developments caused exceeded dust loading. Furthermore, an absent of winter precipitation at the Tien Shan caused increased dust loading
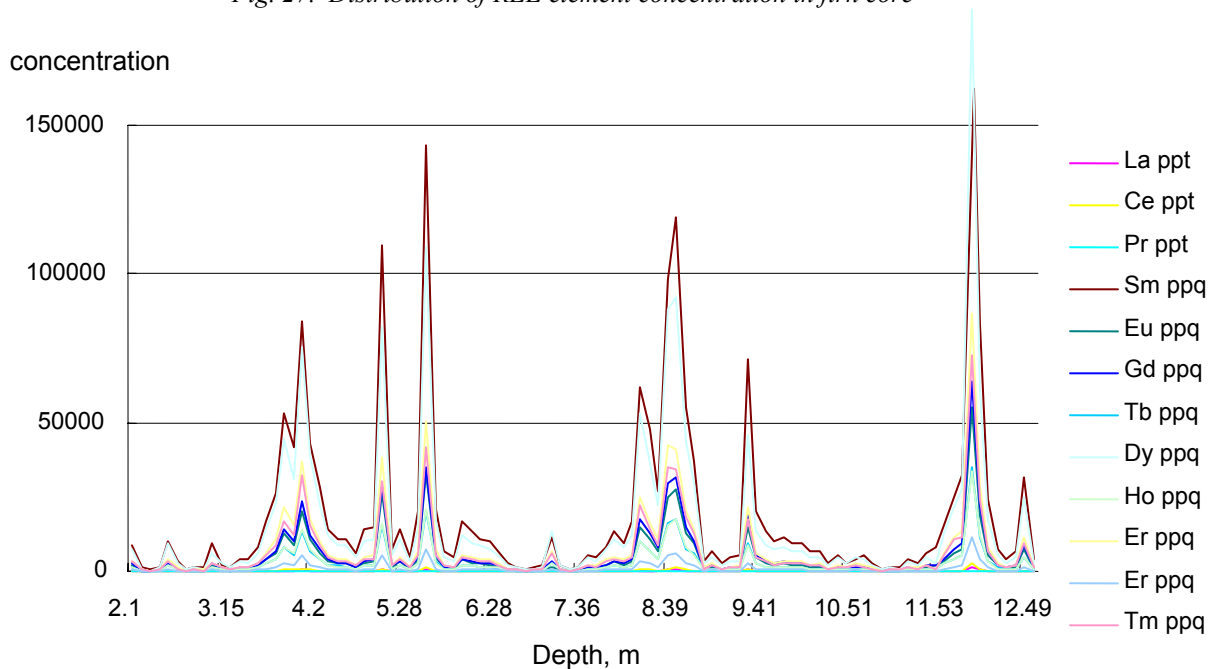
REE concentration

22
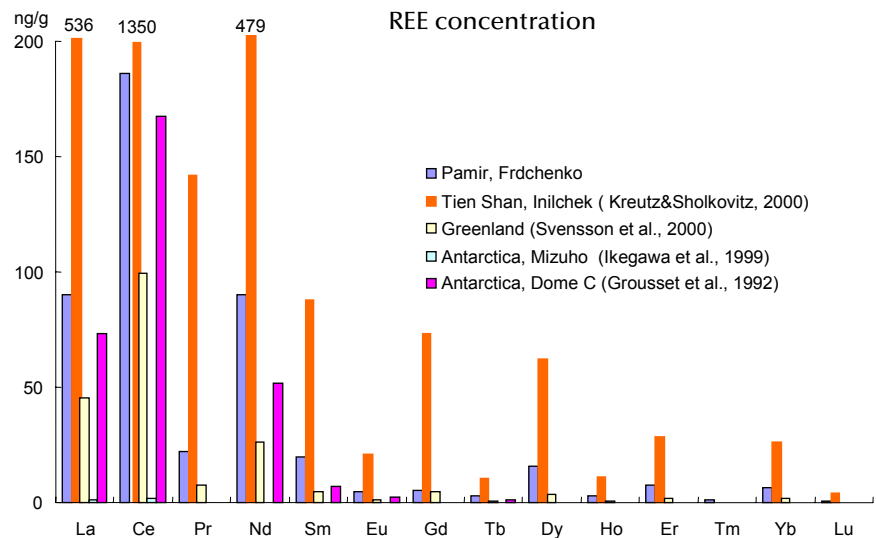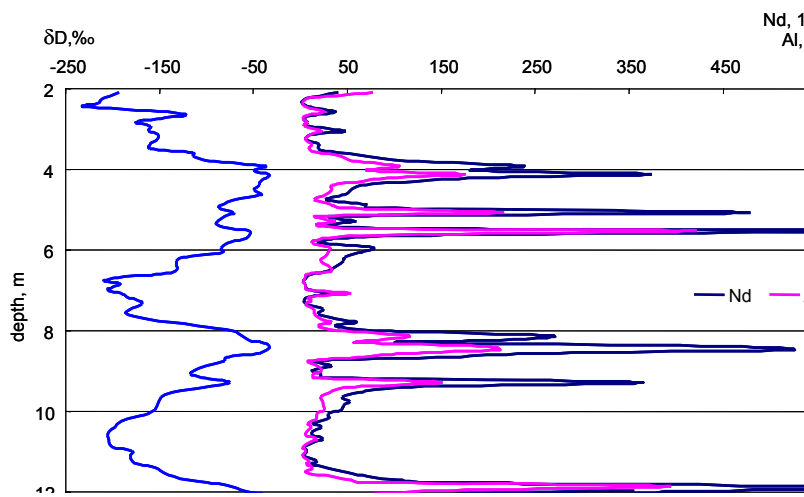
there, while At the Fedchenko, snow accumulated all year around with maximum in winter and spring seasons. However, REE element concentrations from the Pamir, Fedchenko is greater than from Greenland and Antarctic polar plateaus samples.

There is substantial seasonal variability in the deposition of mineral dust as illustrated by the depth profile of Al, Fe (not shown) Nd and even Ca displaying identical to $\delta^{18}O$ (not shown) and $\delta D$ stable isotope down core changes with several maximum peaks in summer and background minimum dust conditions in winter (Fig. 26).

The difference between background and high dust conditions is large, e.g., for Nd 1118-17 pg/g; for Al: 395 – 17 ng/g; for Ca 3171 – 12 ng/g. There are two maximums in stable isotope and mineral dust distribution during warm season each year that could be explained by intrusions of western originated cyclones and Indians monsoons.

*Fig. 27. Distribution of REE element concentration in firn core*



The S profile is not always mirror of those of Al, Nd and Ca (Fig. 26). Dusts of different composition are deposited at different times, especially for Ca and S concentration. The similarity in REE patterns suggest that losses is the predominant lithogenic material transported to the Pamir (Fig. 27).

Loess composition is responsible for changes in Nd(Neodymium) /Yb (Ytterbium) ratio. Low Nd/Yb samples represent input of non-loess dust. As bigger ratio as bigger loess input (Zhang et al., 1998). There is substantial seasonal variability in Nd/Yb ratio corresponding to seasonal variability in

stable isotope profile (Fig. 28) with maximum befor maximum in $\delta^{18}O$ (air temperatures), e.g., at the beginning of summer. Well known regional wind called 'Afghanis' developing in June is bringing loess from Iran, Afghanistan and Tajikistan.
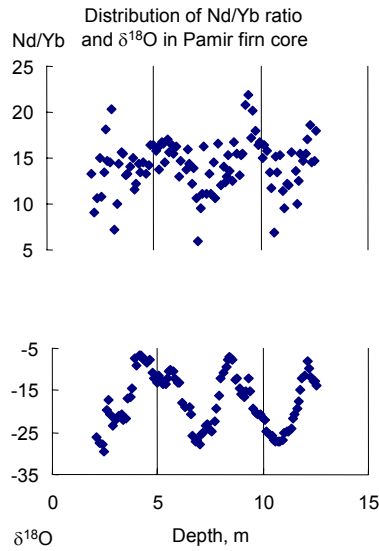


*Fig. 28. Seasonal variability in Nd/Yb ratio corresponding to seasonal variability in stable isotope profiles.*
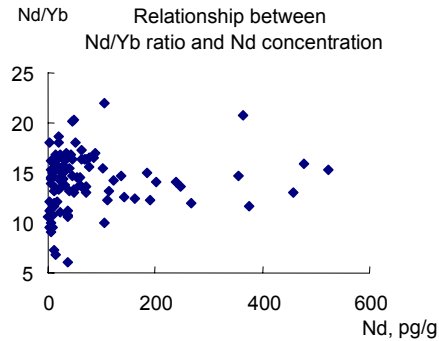
Table 1 Element Ratios in the Fedchenko Glacier core samples and central Asian aerosols

|  | Fedchenko | * |  |
|---|---|---|---|
| Fe/Al | 1.07 | 1.06 | E. China dust (Zhang et al., 1993) |
| Ca/Al | 6.52 | 6.1 | Inilchek (Kretz and Sholkovitz, 2000) |
| Ca/S | 4.28 | 3.95 | Tajik (Gomes and Gillette, 1992) |
| Fe/S | 0.70 | 1.78 | Tajik (Gomes and Gillette, 1992) |
| La/Sm | 4.48 | 4.43 | China sediments, quaternary deposition (Taylor&McLennan, 1985) |
|  | Fedchenko | * |  |
| Fe/Al | 1.07 | 1.06 | E. China dust (Zhang et al., 1993) |
| Ca/Al | 6.52 | 6.1 | Inilchek (Kretz and Sholkovitz, 2000) |
| Ca/S | 4.28 | 3.95 | Tajik (Gomes and Gillette, 1992) |
| Fe/S | 0.70 | 1.78 | Tajik (Gomes and Gillette, 1992) |
| La/Sm | 4.48 | 4.43 | China sediments, quaternary deposition (Taylor&McLennan, 1985) |

*\* Most closest values from central Asian aerosols.*

---

# ATTENTION TO DOE/INL

Ice cores from middle- and low-latitude glaciers can provide annual records of past climate and chemistry of the atmosphere extending back many millennia. Study of these records is essential to discovering the climatic and environmental conditions in which humankind developed and how these changes may affect our future. However, glaciers suitable for study in mid-

and low-latitudes of North America have disappeared during the last 150-200 years. Fortunately, there are Eurasian and South American high elevation glaciers where we can still recover climatic and environmental signals relating to past climate, de- and reforestation, volcano eruptions, biomass burning, permafrost freezing and thawing, and atmospheric pollution related to aeolian erosion and deposition, and increasing anthropogenic emissions in time of industrial boom.

Among of paleo-climatic data, only high resolution ice-core records present the proxy information on hundreds to hundreds of thousand years in natural variations to simulate possible consequences of climate changes for the Earth's population. Isotope-temperature data recovered from ice-core records correlates much better with the instrumental records than what is available from tree ring, marine, or lake sediment derived temperature proxy, but such data can only be obtained through specialized research expeditions to mid- and low-latitude glaciers.

**Accomplishments**
Recovery of ice cores from alpine sites can be accomplished by small, highly experienced teams at a fraction of the cost of polar ice coring projects. This type of research at glaciers over 6000 m above sea level requires highly specialized teams and equipment. Only three such teams exist in the U.S. Three years ago the University of Idaho team joined with the University of Maine to work together. The Ice-core Climate Archive Recovery Activity (ICARA) initiated by the UI-UM team is intended address the need for more middle- to low-latitude ice core collection, analysis, and interpretation and integration of these records with polar ice core records.

This team has become one of the top teams in the World for mid- to low-latitude ice-coring paleo-climatic research. Between 1998 and 2003, four deep ice-cores (160-180 m each) and six shallow firn cores (20-25 m each) have been recovered in central Asia (Tien Shan, Altai, Tibet). Hundreds of snow, precipitation, and water samples have been collected, and the team has measured glaciological and topographic information on the glaciers. Borehole temperature records, year-round meteorological observations, long-term hydro-meteorological data, and water chemistry data have been collected and analyzed.

In 2002 and 2003 an ice-core laboratory and ice-core storage freezers were built to store and process ice-cores. Two new mass-spectrometers for stable isotope analysis, light-weight sun-powered electromechanical ice-coring drill, three automatic weather stations, mountaineering gear for work at high altitudes, and other necessary scientific tools and equipment have been purchased for research. Research thus far has produced 30 scientific papers

and 17 professional presentations in the U.S. and at European scientific meetings. Six undergraduate and four graduate students were trained and graduated from this program between 2001 and 2005, and two PhD students continue to work on their theses.

## Obstacle

**This work was previously funded by the U.S. Department of Energy and Idaho National Laboratory (previously Idaho National Environmental and Engineering Laboratory). However, in 2004 the US DOE and INL discontinued financial support of this research due to the structural reorganization and scientific reorientation. Cessation of funding has suspended these unique investigations at the University of Idaho.**

**Opportunity** The team now develop an international Central Asia Deep Ice-Coring Project (CADIP) in collaboration with institutions in Japan, Germany, Switzerland, France, China, Russia, Tajikistan and Kyrgyzstan to recover the deepest ice core in the World (1000 m) in the Pamir mountains in 2008-2009 and several other surface to bottom ice-cores from Tien Shan, Tibet, and the Andes in the next 5-7 years. This unique, collaborative research is poised to proceed, but lacks sufficient funding. The UI research team is very much disappointed of no attention to this research from DOE/INL while this Project was initially created by this Agency and the Idaho National Laboratory.

**Thus we very much appreciate your attention in continuing support for this unique research by providing a federal framework and increased resources to develop a more comprehensive understanding about the risks and possible effects of rapid change in our world's climate.**

Prof., Dr. Vladimir Aizen
CADIP Leader and Chief Scientist